

See discussions, stats, and author profiles for this publication at: <https://www.researchgate.net/publication/221769523>

# Development of a New Flow Reactor for Kinetic Studies. Application to the Ozonolysis of a Series of Alkenes

ARTICLE in THE JOURNAL OF PHYSICAL CHEMISTRY A · FEBRUARY 2012

Impact Factor: 2.69 · DOI: 10.1021/jp211480x · Source: PubMed

CITATIONS

3

READS

42

6 AUTHORS, INCLUDING:



**Duncianu Marius**

Université Paris-Est Créteil Val de Marne - Univ...

8 PUBLICATIONS 22 CITATIONS

SEE PROFILE



**Véronique Riffault**

Ecole Nationale Supérieure des Mines de Douai

46 PUBLICATIONS 255 CITATIONS

SEE PROFILE



**Alexandre Tomas**

Ecole des Mines de Douai

41 PUBLICATIONS 241 CITATIONS

SEE PROFILE



**Patrice Coddeville**

Ecole des Mines de Douai

55 PUBLICATIONS 403 CITATIONS

SEE PROFILE

# Development of a New Flow Reactor for Kinetic Studies. Application to the Ozonolysis of a Series of Alkenes

Marius Duncianu,<sup>†,‡</sup> Romeo Iulian Olariu,<sup>§</sup> Véronique Riffault,<sup>\*,†,‡</sup> Nicolas Visez,<sup>†,||</sup> Alexandre Tomas,<sup>†,‡</sup> and Patrice Coddeville<sup>†,‡</sup>

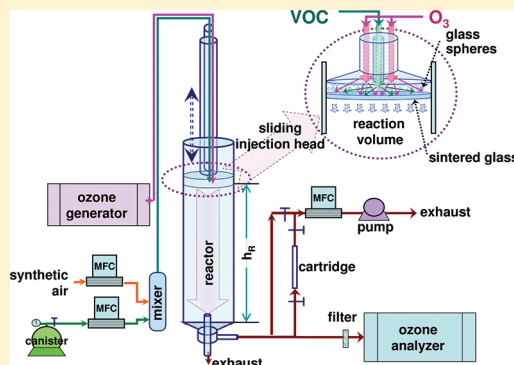
<sup>†</sup>Université Lille Nord de France, F-59000, Lille, France

<sup>‡</sup>EMDouai, CE, F-59508 Douai, France

<sup>§</sup>Faculty of Chemistry, "Al. I. Cuza" University of Iasi, 11 Carol I, 700506, Iasi, Romania

<sup>||</sup>Physico-Chimie des Processus de Combustion et de l'Atmosphère, UMR CNRS 8522, Université de Lille 1, 59655 Villeneuve d'Ascq, France

**ABSTRACT:** A new flow reactor has been developed to study ozonolysis reactions at ambient pressure and room temperature ( $297 \pm 2$  K). The reaction kinetics of  $O_3$  with 4-methyl-1-pentene (4M1P), 2-methyl-2-pentene (2M2P), 2,4,4-trimethyl-1-pentene (tM1P), 2,4,4-trimethyl-2-pentene (tM2P) and  $\alpha$ -pinene have been investigated under pseudo-first-order conditions. Absolute measurements of the rate coefficients have been carried out by recording  $O_3$  consumption in excess of organic compound. Alkene concentrations have been determined by sampling adsorbent cartridges that were thermodesorbed and analyzed by gas-chromatography coupled to flame ionization detection. Complementary experimental data have been obtained using a 250 L Teflon smog chamber. The following ozonolysis rate coefficients can be proposed (in  $cm^3 \text{ molecule}^{-1} \text{ s}^{-1}$ ):  $k_{4M1P} = (8.23 \pm 0.50) \times 10^{-18}$ ,  $k_{2M2P} = (4.54 \pm 0.96) \times 10^{-16}$ ,  $k_{tM1P} = (1.48 \pm 0.11) \times 10^{-17}$ ,  $k_{tM2P} = (1.25 \pm 0.10) \times 10^{-16}$ , and  $k_{\alpha\text{-pinene}} = (1.29 \pm 0.16) \times 10^{-16}$ , in very good agreement with literature values. The products of tM2P ozonolysis have been investigated, and branching ratios of  $(21.4 \pm 2.8)\%$  and  $(73.9 \pm 7.3)\%$  have been determined for acetone and 2,2-dimethyl-propanal, respectively. Additionally, a new nonoxidized intermediate, 2-methyl-1-propene, has been identified and quantified. A topological SAR analysis was also performed to strengthen the consistency of the kinetic data obtained with this new flow reactor.



## INTRODUCTION

A significant part of the total primary volatile organic carbon (VOC) emissions to the atmosphere is formed by alkenes, and their ozonolysis continues to receive attention, due to its important role in atmospheric chemistry. The alkene ozonolysis rate coefficients are useful as input data for comprehensive atmospheric chemical models describing air quality at urban or regional scales, where ozonolysis may be the most important sink for alkenes.

Under atmospheric conditions, the reactions of ozone with alkenes provide free radicals and reactive intermediates. Gas-phase ozonolysis reactions involving alkenes can be a significant source of hydroxyl radicals in the atmosphere<sup>1–3</sup> and precursors of carbonyls or carboxylic acids.<sup>4–6</sup>

In this work, we have studied the ozonolysis kinetics of four methylated pentenes, i.e., 4-methyl-1-pentene (4M1P), 2-methyl-2-pentene (2M2P), 2,4,4-trimethyl-1-pentene (tM1P), 2,4,4-trimethyl-2-pentene (tM2P), and  $\alpha$ -pinene in a flow reactor newly developed in our laboratory, aiming to investigate the primary particle formation steps. The literature describes a limited number of flow reactors used in the study of the formation, evolution, or aging of aerosols,<sup>7–16</sup> and the present

study confirms their versatility and the capacity of also using them in kinetic studies.

Some of the alkenes investigated in this work (2M2P and 4M1P) have been identified in common processes such as tailpipe emissions of volatile hydrocarbons from gasoline-powered motor vehicles,<sup>17</sup> residential fireplace combustion of wood,<sup>18</sup> or in natural fires of foliage, litter, and herbaceous matter.<sup>19</sup>  $\alpha$ -Pinene is a well-known biogenic compound that forms secondary organic aerosols (SOA) in the atmosphere following oxidation processes.

It should be pointed out that the four pentenes have been selected for the validation step because their  $O_3$  reaction rate coefficients are already known in the literature; and yet, while  $O_3$  + alkene reaction kinetics and mechanisms are generally investigated in environmental simulation chambers with large reaction times, the present work on the pentenes is to the best of our knowledge the first one carried out at much shorter reaction times.

**Special Issue:** A. R. Ravishankara Festschrift

**Received:** November 29, 2011

**Revised:** January 23, 2012

**Published:** January 23, 2012

Moreover, current uncertainties on such alkene oxidation mechanisms result from the incomplete description of the excited Criegee intermediate decay channels, which determine the extent to which each of these channels generate radicals.<sup>20</sup>  $\alpha$ -Pinene ozonolysis was also studied, since the reaction system is more complex and involves heterogeneous processes due to the formation of SOA.<sup>21,22</sup> Besides the main homogeneous process, the presence of particulate matter could induce supplemental reactions in the particulate phase or adsorptive processes.

To add more confidence to the data obtained with the flow tube, similar kinetic studies have been performed on the pen-tenes using a Teflon bag smog chamber. Finally, a structure–activity relationship (SAR) analysis has been applied to prove the consistency of the obtained results.

## 1. EXPERIMENTAL METHODS

### 1.1. Flow Reactor Setup for Kinetic Measurements.

The new aerosol flow tube is schematically represented in Figure 1. The cylindrical reactor (Pyrex tube with 1 m length

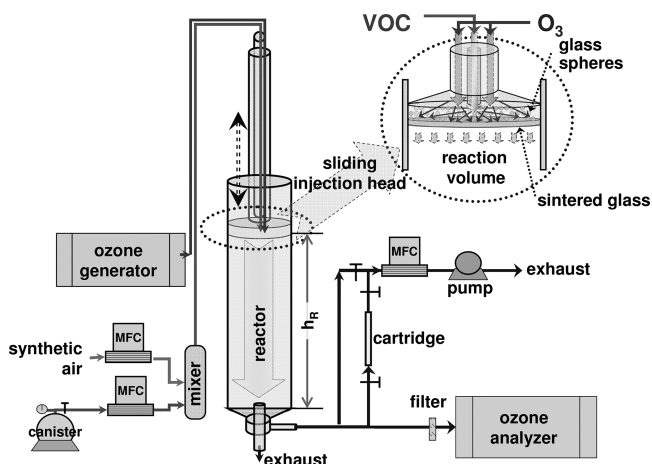


**Figure 1.** Schematic of the experimental setup and instrumentation (MFC: mass flow controller;  $h_R$ : reactor height).

and 10 cm i.d.) has been designed to work with total flows of about 1.5 to 5 L min<sup>−1</sup>, corresponding to reaction times ranging between 30 s and ~5 min. Its vertical position assures a gravitational equilibrium of the flow, and a sliding injector ending with a mixing chamber is used to introduce the reagents

on two different lines and to ensure homogeneity before their entrance into the reaction volume. The passage of the fluid into the reactor is assured by a sintered glass wall welded to the mixing chamber filled with glass beads (diameter: 2 mm), thus providing optimal conditions to rapidly achieve a laminar flow regime. The injection head has been designed to allow good mixing of the reactive gases at transit times of seconds (1–2.5 s) and to support the formation of a laminar flow (Reynolds number,  $Re \sim 20$ –50) in the reactor. The laminar flow in the reactor ensures a stationary mode as a function of the reaction volume, at atmospheric pressure and room temperature ( $T = 297 \pm 2$  K). At the bottom of the reactor, two exhaust lines consisting of 1/4-in. glass tubes are used to collect samples. The central one reaches the laminar flow region roughly 15 cm above the bottom of the reactor. The reactor height is defined by the distance between the injector head and the central sampling point. The volume difference between the central sampling line and the lateral one was taken into account to correct the reaction time for each reactor height.

Both Reynolds ( $Re$ ) and Péclet ( $Pe$ ) dimensionless numbers can be calculated in order to characterize transport phenomena in fluid flows:

$$Pe = \frac{LU}{D} = Re \times Sc \quad (1)$$

where  $L$  is the characteristic length,  $U$  is the average velocity,  $D$  is the mass diffusion coefficient, and  $Sc$  is the Schmidt number equal to the ratio between the kinematic viscosity and  $D$ . For all experiments, the Péclet numbers were inferior to 50, indicating nonplug flows.<sup>23</sup>

A pulse tracer study similar to previous approaches<sup>24</sup> was performed using either  $O_3$  or  $CO$  to validate the calculation of the contact time into the reactor (which is defined as the ratio between the reactor height,  $h_R$ , and the average velocity). The velocity profile in laminar flow conditions presents a parabolic distribution (zero at the wall, maximum at the center of the reactor), implying that tracer molecules traveling at the center of the cylinder will be detected first, while the average velocity will correspond to the time of the first derivate ( $dO_3/dt$ ) maximum. The concentration profiles of the tracer analytes were monitored with 1 s time resolution measurements using spectroscopic analyzers (Models 48C and 49C, Thermo Environmental Instruments) for various heights of the reactor and several characteristic flows. The example given in Figure 2a

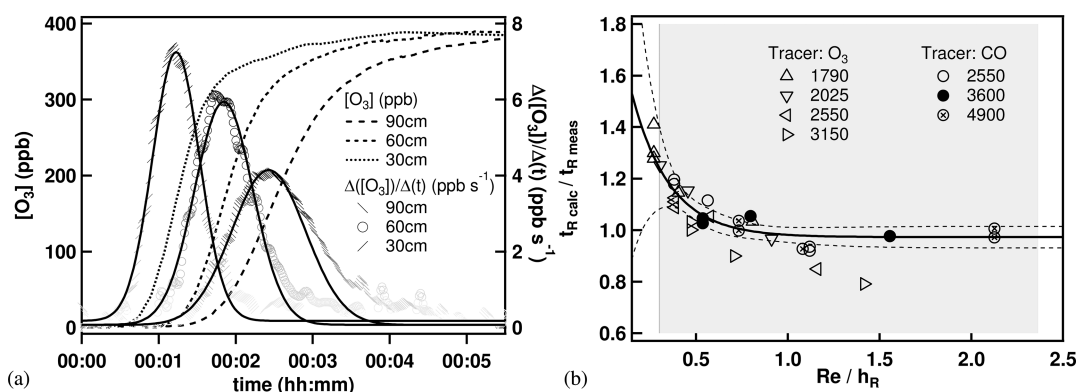


**Figure 2.** (a) Concentration profiles of ozone used as a tracer analyte to characterize the reactor flow for three reactor heights. (b) Correction factor between the calculated average residence time ( $t_{R,calc}$ ) and the measured residence time ( $t_{R,meas}$ ) for several heights of the reactor ( $h_R$ ) and several characteristic bulk flows (in mL min<sup>−1</sup>) in the reactor in laminar flow conditions using two tracers. The broad line is the exponential regression fit of all the data, while the dotted lines represent the 95% confidence interval. The gray area represents the  $Re/h_R$  range of all the kinetic measurements.

shows the ozone time profiles and their first derivatives ( $\Delta[\text{O}_3]/\Delta t$ , which were fitted using Gaussian curves) for a  $3150 \text{ mL min}^{-1}$  flow. The average bulk velocity was corrected using the ratio between the calculated residence time,  $t_{R\_calc}$  as derived from the laminar flow theory and the measured residence time,  $t_{R\_meas}$ , spanning from 28 to 177 s for the tracer study. The ratio was close to unity for the most part of the flow range (described by  $Re$ , values ranging from 20 to 64 for the tracer study) whatever the reactor heights ( $h_R$ , expressed in cm), as seen in Figure 2b. The gray area represents the  $Re/h_R$  range of all the kinetic measurements. The response time of the tracer analyzer and the diffusion coefficient of the analyte due to the concentration gradient were taken into account to correct the estimation of the measured residence time. The diffusion correction was under 5% for most experiments and never exceeded 10%.

For alkene ozonolysis, a continuous gas flow of the selected VOC is achieved using a pressurized canister, with a few milliliters per minute being released through a mass flow controller (MFC) in a premixing chamber. Purified air is used as a carrier gas and ensures the dilution of the VOC at the requested level of concentration. On the other hand, an ozone generator (Model 146i, Thermo Scientific) provides a controlled flow of oxidant which reaches the injection head via a separate line. The controlled flows of ozone and volatile organic compound enable predefined and stable concentrations at the top of the reactor to be obtained.

The volume of the flow reactor can be modified by moving up and down the sliding injection head, thus allowing one to monitor the evolution of the reagents and products at various reaction times and to estimate kinetic and mechanistic parameters. Different reaction times may also be achieved by changing the total flow rate for a given distance between the movable injection head and the sampling outlet.

The side line was used to sample adsorption cartridges, to determine the ozone concentration and evacuate the main flow, while the central one will be used in further studies for aerosol sampling in isokinetic conditions. The cartridges filled with three different adsorbents (Carbopack C, Carbopack B, and Carbosieve SIII in 1:2:1 packing ratio from Supelco) were sampled at  $50 \text{ mL min}^{-1}$  before injecting ozone to determine the initial concentration of the VOC in excess. A cartridge bypass was installed to continuously purge the Teflon line with the exhaust air of the reactor before and after sampling. The reactant concentration was estimated using calibration curves obtained with cartridges doped with known concentrations of analytes. Six cartridges were sampled in the absence of ozone at different heights in the reactor to check for the concentration of the organic reactant, the potential wall losses (found negligible for all compounds), as well as the reproducibility and accuracy of the sampling. It should be noted that in the presence of ozone, a KI-coated copper tube upstream from the sampling cartridge was used as a denuder to avoid the loss of the alkenes through  $\text{O}_3$  reaction on the adsorbent.<sup>25</sup>

For the kinetic experiments in the flow reactor, sampled cartridges were then thermally desorbed (within 24 h) in a two-stage thermodesorber (Markes Unity2) and analyzed by GC/FID (Agilent 7890A). A Varian capillary column (CP-Sil 5 CB 50 m, 0.32 mm,  $1.2 \mu\text{m}$ ) was used with the following temperature program:  $35^\circ\text{C}$ , 15 min isothermal,  $4^\circ\text{C min}^{-1}$  to  $125^\circ\text{C}$ , then  $20^\circ\text{C min}^{-1}$  to  $250^\circ\text{C}$  and held for 6 min. Helium was used as the carrier gas with a column flow of  $\sim 3 \text{ mL min}^{-1}$ .

Initial concentrations in the flow reactor were (0.81–8.1)  $\text{ppm}_v$  for the alkene ( $1 \text{ ppm}_v = 2.46 \times 10^{13} \text{ molecules cm}^{-3}$  at 298 K and 1 atm) and (61–374)  $\text{ppb}_v$  for ozone.

The outlet analytical chain includes an online  $\text{O}_3$  analyzer (Model 49C, Thermo Environmental Instruments) based on UV absorption spectroscopy. The absence of interferences coming from the alkenes investigated in the present study were checked by considering their UV absorption spectra, as well as by measurement tests in the absence of ozone. As for possible interferences from the ozonolysis products, alkene concentrations were increased progressively until the total consumption of ozone in the reactor was reached, while the  $\text{O}_3$  analyzer presented a background value similar to the background value of purified air.

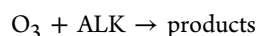
**1.2. Smog Chamber Setup.** In order to obtain additional confirmation of the kinetic parameters obtained with the aerosol flow reactor, complementary experiments were performed on the four pentenes in a smog chamber that has been described previously.<sup>26</sup> Only the aspects specific to the current experiments are presented below.

The reaction chamber consists of a Teflon bag with a volume of about 250 L working at atmospheric pressure,  $(297 \pm 2) \text{ K}$ , and in the dark. Teflon tubes are used for the introduction of the reactants and the sampling by the analytical instruments. Ozone was produced by flowing purified air through a UV lamp ozonizer (Model 165, Thermo Environmental Instrument), which was directly injected in the Teflon chamber at a flow rate of about  $2.8 \text{ L min}^{-1}$ . The ozone concentration was determined as a function of reaction time by using an online ozone analyzer (Model 41M, Environnement S.A.) with a time resolution of about 20 s. The analyzer sampling flow rate and precision were  $0.90 \text{ L min}^{-1}$  and 5  $\text{ppb}$ , respectively. Initial  $\text{O}_3$  concentrations in the reaction chamber were in the range 70–300  $\text{ppb}_v$ .

All the investigated alkenes being liquid reagents, they were injected with microliter syringes into a small heated glass cell placed on a secondary input line of clean air in order to ensure a complete and rapid evaporation. Initial alkene concentrations – calculated by taking into account the injected volume of alkene and the total volume of the bag – were in the range 1.1–3.4  $\text{ppm}_v$ . Additional control experiments were carried out to check the stability of the reactants in the Teflon bag, showing that all the selected olefins and  $\text{O}_3$  do not suffer any significant wall losses while in the chamber.

In a typical experiment, ozone was first added into the Teflon bag. At time zero, the pentene was injected in the reactor using a high flow of purified air ( $\sim 15 \text{ L min}^{-1}$ ), thus ensuring a rapid dilution of the organic reactant in the ozone-containing Teflon chamber. For each investigated compound, one experiment was performed using cyclohexane as an OH scavenger, and no significant difference was observed in the ozone decay and, therefore, in the ozonolysis rate coefficient.

**1.3. Absolute Rate Measurements. Kinetic Determination Formalism.** Rate coefficients for the investigated ozone reactions were determined in both reactors by monitoring the  $\text{O}_3$  decay rates in the presence of excess and known concentrations of the alkene (ALK). As the ozone loss caused by wall deposition was shown to be negligible, the temporal profile of  $\text{O}_3$  is governed by a unique process:



leading to the following rate equation:

$$-\text{d} \ln[\text{O}_3]_t / \text{d}t = k_{\text{ALK}} \times [\text{O}_3]_t \times [\text{ALK}]_t \quad (\text{II})$$



where  $[ALK]_t$  and  $[O_3]_t$  are the concentrations in alkene and ozone at time  $t$  and  $k_{ALK}$  is the ozonolysis rate coefficient.

With the initial alkene concentration  $[ALK]_0$  being in excess by at least a factor of 10 over the initial ozone concentration, the alkene concentration remains essentially constant throughout the reaction time. This approximation is only valid if there are no other additional processes, such as competitive reaction, wall loss, or/and OH radical reactions that could contribute to the alkene decay except the ozonolysis.

On the basis of literature data, it is well-known that the reaction of ozone with unsaturated species can produce OH radicals,<sup>2,27–33</sup> which may further react with the organic reactant, resulting in a significant change in the alkene concentration. Complementary experiments were thus performed with cyclohexane (in smog chamber and flow tube experiments) or CO (in flow tube experiments) added as OH scavenger. CO was preferred because it is an effective scavenger of OH<sup>34,35</sup> without causing interference in the product study. After data evaluation for experiments with and without OH scavenger, no significant difference was observed in the rate coefficients given the uncertainties. It should also be noted that the reactions were generally carried out in a large excess of the organic reactant, so that the possible additional loss of the alkene by reaction with OH would have a limited effect on the alkene concentration.

On the basis of the above observations, the pseudo-first-order rate coefficient,  $k'_{ALK}$ , may be introduced as

$$k'_{ALK} = k_{ALK} \times [ALK]_0 \quad (\text{III})$$

Equation II becomes

$$-d \ln [O_3]_t / dt = k'_{ALK} \times [O_3]_t \quad (\text{IV})$$

Integrating the rate law yields

$$\ln([O_3]_0/[O_3]_t) = k'_{ALK} \times t \quad (\text{V})$$

According to the last relation, the slope of the linear fitting of  $\ln([O_3]_0/[O_3]_t)$  versus  $t$  gives the pseudo-first-order rate coefficient  $k'_{ALK}$ , whose value can be divided by the initial alkene concentration to retrieve the ozonolysis rate coefficient  $k_{ALK}$  through eq III.

Additional experiments were performed, in the case of  $\alpha$ -pinene, in reversed conditions, i.e., in excess of  $O_3$  and monitoring the decay rates of  $\alpha$ -pinene. Though giving complementary results, this strategy was not pursued since the approach was more time-consuming and generated higher uncertainties in the  $\alpha$ -pinene concentrations (and thus in the  $k'$  values) as compared with the general case described above.

**1.4. Product Study in the Flow Reactor.** Because of its higher rate coefficient and the fact that the double bond is not located on a terminal carbon, which facilitates product identification with the available analytical techniques, tM2P was chosen to validate the flow reactor from a mechanistic point of view.

The alkene ( $[tM2P]_0 = (3.9\text{--}4.3) \times 10^{12}$  molecules  $\text{cm}^{-3}$ ) and ozone ( $[O_3]_0 = 5.1 \times 10^{12}$  molecules  $\text{cm}^{-3}$ ) were introduced into the flow reactor in the presence of carbon monoxide ( $[CO]_0 = 3 \times 10^{16}$  molecules  $\text{cm}^{-3}$ ) as the OH radical scavenger. A total flow of 900  $\text{mL min}^{-1}$  was chosen in order to obtain greater reaction times, required to ensure the conversion of a sufficient amount of reagents at the sampling time.

Since the sampling rate of the ozone analyzer ( $1300 \text{ mL min}^{-1}$ ) is higher than the total flow rate, an additional amount of dry

air was added in the reactor flow during ozone level measurements, and its concentration was corrected for dilution.

Gaseous samples were collected online (Thermo Desorption System, Gerstel) on adsorbent tubes kept at  $0^\circ\text{C}$ , trapping the volatile organic compounds at a rate of  $50 \text{ mL min}^{-1}$  for a total volume of 500 mL. Once collected, the analytes are thermodesorbed and transferred toward a cryogenic trapping (Cooled Injection System, CIS) capillary tube of small diameter (2 mm) filled with a few milligrams of adsorbent (Carbopack B,  $\sim 8 \text{ mg}$ ) to focus analytes before entering the chromatographic column. The chromatographic and spectrometric analysis was further performed by a GC/FID-MS (Agilent 6890N/5975B) instrument equipped with a DB-5 ms (123–5563;  $60 \text{ m} \times 0.32 \text{ mm}$ ,  $1 \mu\text{m}$ ) column. The separation was carried out at a  $4 \text{ mL min}^{-1}$ , 22.1 psi, He carrier flow. The temperature program was started in cryogenic conditions at  $0^\circ\text{C}$  hold for 5 min, followed by a  $3^\circ\text{C min}^{-1}$  ramp until  $90^\circ\text{C}$  and a steep ramp of  $20^\circ\text{C min}^{-1}$  up to  $250^\circ\text{C}$  (5 min hold).

Reproducibility and breakthrough volume tests were equally performed in the absence of ozone and in ozonolysis conditions for different sampling volumes. The results showed an excellent correlation between the sampling volume and the quantity of analyte as measured by the flame ionization detector (FID) ( $r^2 > 0.998$ ) with a slope value greater by more than 1 order of magnitude than the value of the intercept, suggesting the absence of breakthrough and adsorbent rinsing effects.

**1.5. Reagents.** Chemicals were all commercially available and used as received without further purification.  $\alpha$ -Pinene (>98%), 4M1P (98%), 2,2-dimethyl-propanal (96%), acetone (>99.8%), and cyclohexane (99.5%) were purchased from Sigma-Aldrich. 2-Methyl-1-propene (10 ppm in  $N_2$ ) was purchased from Messer-Griesheim. tM2P (>98%), tM1P (99%), and 2M2P (>99%) were from Janssen Chimica.

Purified air was produced by an air purifier (AZ 2020, Claind) and was characterized by a relative humidity of less than 5% and an organic carbon content of max. 0.1 ppb<sub>v</sub>.

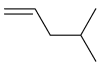
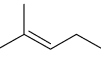
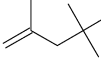
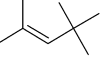
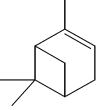
## 2. RESULTS AND DISCUSSION

**2.1. Pentenes: Ozonolysis Rate Coefficients.** The alkene compounds investigated in the present study were chosen in order to fill a wide range of rate coefficient values as a certification of the versatility of the flow reactor. In addition, literature data were available for these alkenes (at least one study). Experimental conditions and results for both reactors are presented in Table 1. Plots of  $\ln([O_3]_t/[O_3]_0)$  versus time obtained with the flow reactor are displayed in Figure 3 for each of the four pentenes investigated at different initial concentrations. The uncertainties ( $1\sigma$ ) quoted in the graphs of Figure 3 represent the sum of the variation coefficients ( $V \equiv s_x/\bar{x}$ , where  $s_x$  is the standard deviation of a set of samples  $x_i$  and  $\bar{x}$  is its mean) of the recorded series of values for  $[O_3]_0$  and  $[O_3]_t$  as derived from the equation

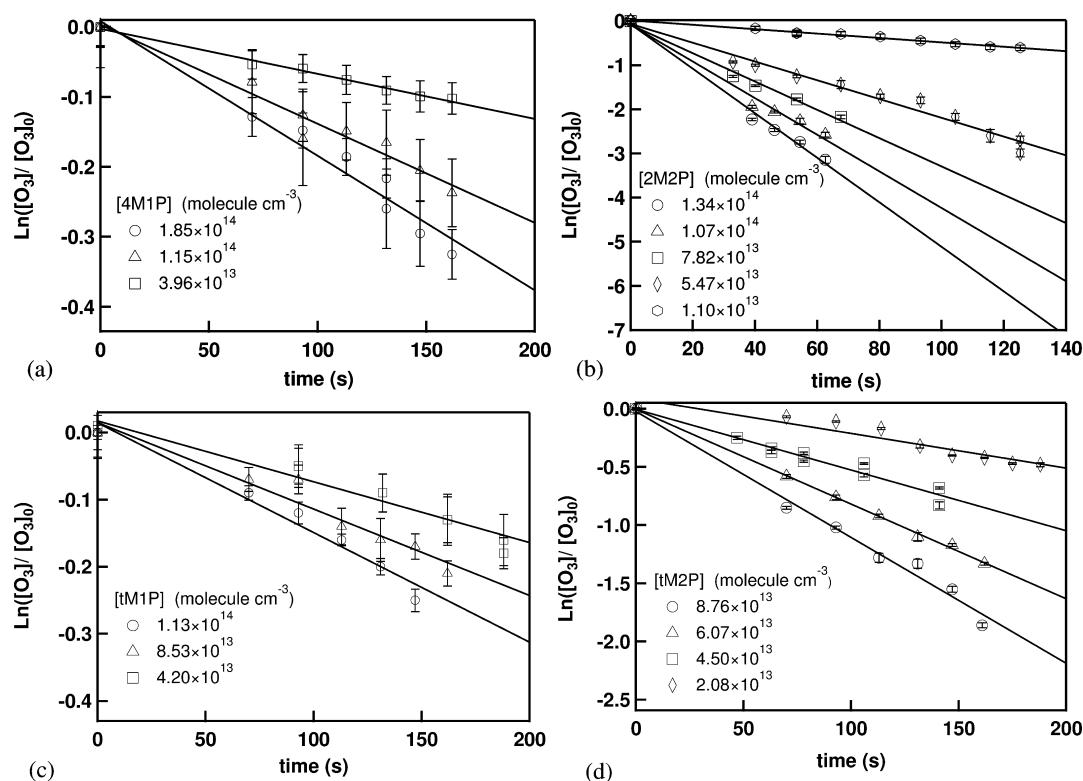
$$\sigma \left\{ \ln \left( \frac{[O_3]_0}{[O_3]_t} \right) \right\} = \sqrt{\left( \frac{\sigma[O_3]_0}{[O_3]_0} \right)^2 + \left( \frac{\sigma[O_3]_t}{[O_3]_t} \right)^2 + 2 \times \frac{\sigma[O_3]_0}{[O_3]_0} \times \frac{\sigma[O_3]_t}{[O_3]_t}} \quad (\text{VI})$$

Nonweighted linear least-squares fits of the data yielded high correlation coefficients and near-zero intercepts, and

**Table 1.** Experimental Conditions and Results Obtained for the Ozonolysis Reactions in Excess of Alkenes at Ambient Temperature and Pressure

Alkene		T (K)	Reactor	no. of	[ALK] <sub>0</sub>	[O <sub>3</sub> ] <sub>0</sub>	k' <sub>ALK</sub>	k <sub>ALK</sub> <sup>d</sup>
Name (Abbreviation)	Structure		type <sup>a</sup>	decays	(× 10 <sup>13</sup> molecule cm <sup>-3</sup> )	(× 10 <sup>12</sup> molecule cm <sup>-3</sup> )	(× 10 <sup>-3</sup> s <sup>-1</sup> )	(× 10 <sup>-17</sup> cm <sup>3</sup> molecule <sup>-1</sup> s <sup>-1</sup> )
4-methyl-1-pentene (4M1P)		297	FR	3	4.0 – 18.5	2.9 – 3.0	0.64 – 1.92	0.823 ± 0.010
			SC	7	3.6 – 10.0	1.9 – 5.0	0.35 – 0.89	
2-methyl-2-pentene (2M2P)		297	FR	5	1.1 – 13.4	1.3 – 9.2	5.0 – 50.4	45.4 ± 1.2
			SC	8	1.9 – 8.4	2.0 – 4.9	10.3 – 34.0	
2,4,4-trimethyl-1-pentene (tM1P)		297	FR	3	4.2 – 11.3	1.5 – 3.4	0.91 – 1.63	1.481 ± 0.012
			SC	7	2.7 – 6.5	2.5 – 4.4	0.34 – 0.99	
2,4,4-trimethyl-2-pentene (tM2P)		297	FR	4	2.1 – 8.8	1.4 – 3.5	3.0 – 10.8	12.50 ± 0.21
			SC	6	1.5 – 6.5	1.9 – 5.1	2.1 – 8.0	
α-pinene		298	FR	9 <sup>b</sup>	1.4 – 10.1	2.0 – 6.2	1.9 – 12.2	12.94 ± 0.35
				2 <sup>c</sup>	0.02 – 0.04	33.7 – 64.5	3.7 – 7.1	

<sup>a</sup>SC: smog chamber; FR: flow reactor. <sup>b</sup>Experiments in excess of alkene. <sup>c</sup>Experiments in excess of ozone. <sup>d</sup>Slope of the weighted linear least-squares fit forced through zero for flow reactor and smog chamber data; the uncertainty was calculated at the 95% confidence level and only represents statistical uncertainty.

**Figure 3.** Plots of ozone consumption versus time for (a) 4M1P, (b) 2M2P, (c) tM1P, and (d) tM2P in the flow reactor experiments.

the slopes led to the pseudo-first-order rate coefficients  $k'_{ALK}$ , where quoted uncertainties correspond to the  $1\sigma$  precision of the fit.

Plotting  $k'_{ALK}$  versus  $[ALK]_0$  for the flow reactor (open marks) and the Teflon chamber (full marks) data (Figure 4) gives the ozonolysis rate coefficients,  $k_{ALK}$ , for all the target compounds, according to eq III. The uncertainties in Figure 4 represent one standard deviation ( $1\sigma$ ) for both axes where the

errors on concentrations correspond to  $1\sigma$  (repeatability) for flow reactor data, and was calculated using the following equation for smog chamber data:

$$\sigma_{ALK} = \sqrt{\left(\frac{\rho_{ALK}}{M_{ALK}} N_A\right)^2 \left( \frac{\sigma_{V_i}^2}{V_{total}^2} + \frac{V_i^2}{V_{total}^4} \sigma_{V_{total}}^2 \right)} \quad (VII)$$

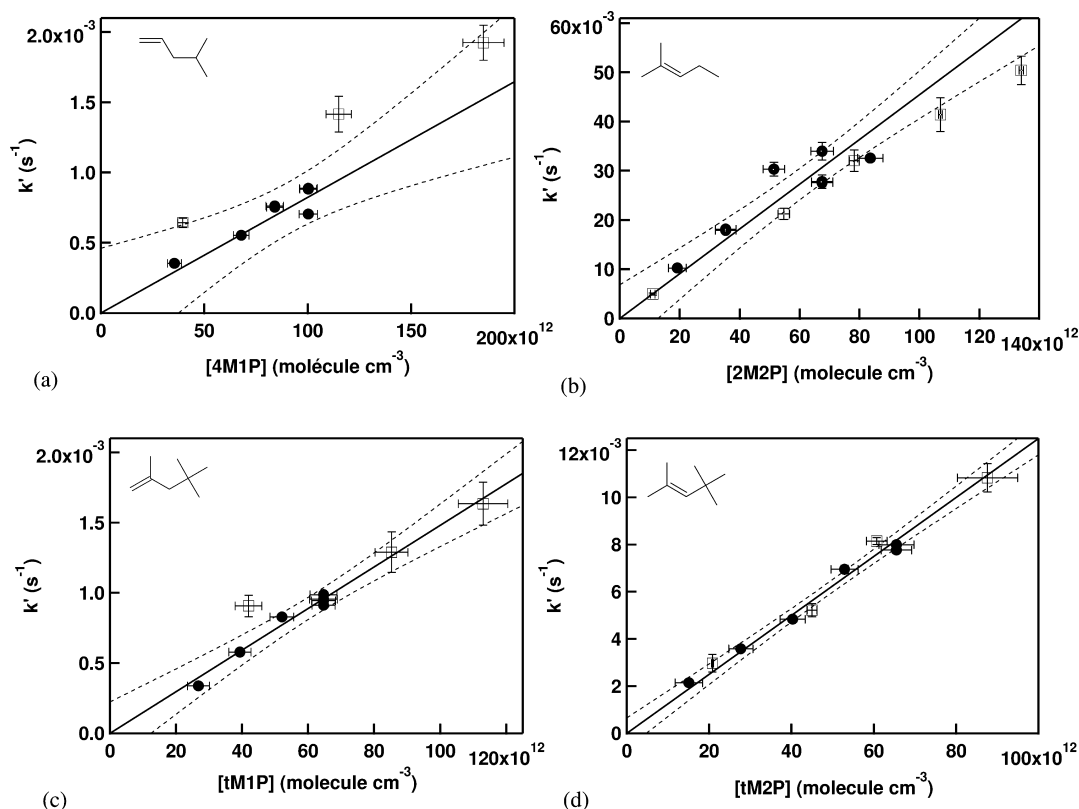


**Figure 4.** Plots of the pseudo-first-order rate coefficient  $k'_{\text{ALK}}$  versus alkene concentration for (a) 4M1P, (b) 2M2P, (c) tM1P, and (d) tM2P. Open squares: flow reactor experiments; filled circles: smog chamber experiments. Straight lines are linear regression fits of all the data, and curved lines are the 95% confidence intervals.

with  $\rho_{\text{ALK}}$  and  $M_{\text{ALK}}$  being the density and molar mass of the alkene, respectively,  $N_{\text{A}}$  is the Avogadro number,  $V_{\text{i}}$  the injected volume of the compound,  $V_{\text{total}}$  is the total volume of the smog chamber,  $\sigma_{V_{\text{i}}}$  is the precision of the microsyringe, and  $\sigma_{V_{\text{total}}}$  is obtained by propagating uncertainties considering flows and times for filling up the Teflon bag.

Fitting was made taking into account the weighting of the standard deviation on  $k'_{\text{ALK}}$  values. Table 1 shows the  $k_{\text{ALK}}$  values obtained together with the 95% confidence interval (also represented as dashed lines in Figure 4). This error was combined with the one estimated for each compound concentration given the repeatability of the measurements (2M2P: 21%; 4M1P: 6%; tM1P: 7%; tM2P: 8%) to give the overall uncertainty reported in Table 2 for each rate coefficient.

A very good agreement between the kinetic data obtained from two very different systems (flow tube and smog chamber) and for a very wide range of reaction times can be observed for all compounds (Figure 5 and Table 2), as well as a good comparison with literature data (Table 2).

2M2P appears to be the most reactive compound toward ozone among those investigated, which can be explained by the alkyl substituents increasing the activity of the unsaturated bond together with a minimal inhibiting steric effect due to the lack of massive substituents. The rate coefficient derived from the flow tube and the smog chamber experiments ( $k_{2\text{M2P}} = 4.54 \times 10^{-16} \text{ cm}^3 \text{ molecule}^{-1} \text{ s}^{-1}$ ) and the value from McGillen et al. (2008) ( $k_{2\text{M2P}} = 4.06 \times 10^{-16} \text{ cm}^3 \text{ molecule}^{-1} \text{ s}^{-1}$ ) present an excellent agreement. On the contrary, the 4M1P kinetics is the slowest in the studied series ( $k_{4\text{M1P}} = 8.23 \times 10^{-18} \text{ cm}^3 \text{ molecule}^{-1} \text{ s}^{-1}$ ), confirming previous studies that determined

values of  $(7.3 \pm 1.4) \times 10^{-18} \text{ cm}^3 \text{ molecule}^{-1} \text{ s}^{-1}$  at 287 K<sup>36</sup> and  $(7.9 \pm 0.3) \times 10^{-18} \text{ cm}^3 \text{ molecule}^{-1} \text{ s}^{-1}$  at 292 K.<sup>37</sup>

While the compounds with substituted methyl groups at the double bond (2M2P, tM2P) present larger rate coefficients, the compounds with terminal double bond (4M1P, tM1P) are clearly less reactive toward ozonolysis. Thus, the present data support very well the increase of the reactivity of the ozone electrophilic addition at the unsaturated carbon–carbon with the degree of substitution, as stated in the literature.<sup>5,6,38,39</sup> Furthermore, the presence of methyl groups at the vicinal carbon of the double bond reduces the ozonolysis rate coefficient as observed in the comparison between 2M2P and tM2P or tM1P and 2,3,3-trimethyl-1-butene (see Table 4), probably due to the contribution of steric effects.<sup>36</sup> Finally, as also observed in the literature, this reactivity is not strongly influenced by the size of the substituent (comparison between 4M1P and tM1P).

**2.2.  $\alpha$ -Pinene: Ozonolysis Rate Coefficient.** The ozonolysis of  $\alpha$ -pinene is an important source of oxidized species in the atmosphere, which contribute significantly to the atmospheric formation of SOA. The  $\text{O}_3$  reaction rate coefficient has been determined by many previous studies and has been reviewed by Atkinson et al. (2006).<sup>40</sup> The ozonolysis of  $\alpha$ -pinene was carried out only in the flow reactor.

Data were analyzed using the same procedure as described previously for the methylated pentenes. Graphs of  $\ln([\text{O}_3]/[\text{O}_3]_0)$  versus time are presented in Figure 6a for different initial concentrations of  $\alpha$ -pinene in excess. Two experiments were also performed in excess of ozone ( $[\text{O}_3]_0 = 1.4$  and 2.6 ppm<sub>v</sub>). The corresponding slopes have been plotted versus  $[\alpha\text{-pinene}]_0$  or  $[\text{O}_3]_0$  in Figure 6b. A value of  $k_{\alpha\text{-pinene}} = (1.29 \pm 0.16) \times 10^{-16} \text{ cm}^3 \text{ molecule}^{-1} \text{ s}^{-1}$  has been obtained

Table 2. Summary of Results and Comparison with Literature Data

alkene	T (K)	$k_{\text{ALK}} \times 10^{-17}$ ( $\text{cm}^3 \text{ molecule}^{-1} \text{ s}^{-1}$ )	experimental setup <sup>a</sup>	reference
4M1P	296	1.06	SC; O <sub>3</sub> excess; GC/FID	Cox and Penkett (1972) <sup>50</sup>
	287	$0.73 \pm 0.14$	SC; VOC excess; OA	Grosjean and Grosjean (1995) <sup>36</sup>
	292	$0.79 \pm 0.03$	SC; VOC excess; OA	Leather et al. (2010) <sup>37</sup>
	297	$0.92^b$		Leather et al. (2010) <sup>37</sup>
	297	$1.28 \pm 0.09^c$	FR; VOC excess; OA	this work
	297	$0.82 \pm 0.05^c$	SC; VOC excess; OA	this work
	297	$0.823 \pm 0.050^c$	FR and SC; VOC excess; OA	this work
2M2P	295	$40.6 \pm 4.9$	SC; VOC excess; OA	McGillen et al. (2008) <sup>48</sup>
	297	$40.8 \pm 8.6^c$	FR; VOC excess; OA	this work
	297	$46.2 \pm 9.7^c$	SC; VOC excess; OA	this work
	297	$45.4 \pm 9.6^c$	FR and SC; VOC excess; OA	this work
tM1P	290	$0.97 \pm 0.22$	SC; VOC excess; OA	Leather et al. (2010) <sup>37</sup>
	297	$1.47^b$		Leather et al. (2010) <sup>37</sup>
	297	$1.65 \pm 0.15^c$	FR; VOC excess; OA	this work
	297	$1.48 \pm 0.10^c$	SC; VOC excess; OA	this work
tM2P	297	$1.48 \pm 0.11^c$	FR and SC; VOC excess; OA	this work
	297	$13.9 \pm 3.4$	SC; VOC excess; OA	Grosjean and Grosjean (1996) <sup>39</sup>
	297	$13.1 \pm 1.1^c$	FR; VOC excess; OA	this work
	297	$12.4 \pm 1.0^c$	SC; VOC excess; OA	this work
$\alpha$ -pinene	298	9.0	IUPAC data	Atkinson et al. (2006) <sup>40</sup>
	297	$12.9 \pm 1.6^c$	FR; VOC excess; OA	this work

<sup>a</sup>SC: smog chamber; FR: flow reactor; OA: ozone analyzer; GC/FID: gas chromatography/flame ionization detection. <sup>b</sup>Values calculated using the proposed Arrhenius equations at 297 K. <sup>c</sup>Overall uncertainty taking into account the 95% confidence interval on the slope of the weighted linear least-squares fit and the uncertainty on the concentration of the compound in excess using the propagation of uncertainty approach.

for the slope of the weighted linear least-squares fit forced through zero. Figure 6b also shows the IUPAC recommended value of  $9.0 \times 10^{-17} \text{ cm}^3 \text{ molecule}^{-1} \text{ s}^{-1}$  from Atkinson et al. (2006).<sup>40</sup> A repeatability of 12% for  $\alpha$ -pinene concentrations is taken into account for the estimation of the overall uncertainty reported in Table 2. Very good agreement could be observed between the results obtained in excess of  $\alpha$ -pinene and those obtained in excess of ozone. The larger error bars in  $k'_{\alpha\text{-pinene}}$  may be related to the high concentrations of O<sub>3</sub> used, which limits the efficiency of the KI scrubbers used upstream of the sampled cartridge, and thus the repeatability of the measurements.

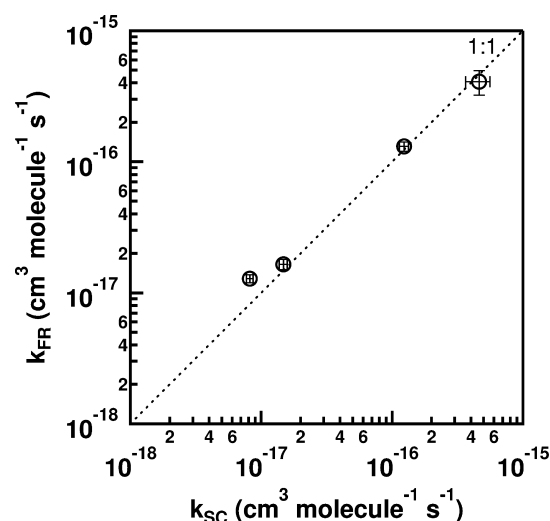


Figure 5. Comparison between the rate coefficients obtained from flow reactor ( $k_{\text{FR}}$ ) and smog chamber ( $k_{\text{SC}}$ ) experiments plotted with their overall uncertainty.

In the case of  $\alpha$ -pinene, the rate coefficient obtained in the present work is in very good agreement with the recommended value.<sup>40</sup> A recent kinetic study<sup>41</sup> involving the use of a similar flow reactor also reports a  $k_{\alpha\text{-pinene}}$  value at the upper limit of the IUPAC recommendation ( $1.1 \pm 0.1 \times 10^{-16} \text{ cm}^3 \text{ molecule}^{-1} \text{ s}^{-1}$ ), consistent with our study.

**2.3. tM2P: Product Study.** Cartridges were sampled at several reaction times in order to follow the formation of the reaction products and the consumption of reagents. As expected, the two main stable oxidation products were identified by comparison with NIST mass spectra as acetone and 2,2-dimethyl-propanal, and their temporal distribution profiles are presented in Figure 7. A 30% consumption of tM2P was observed at the maximum reaction time. For all reaction times, there is a close-to-unity sum of the branching ratios ( $95.3 \pm 5.2\%$  on average), with mean yields of ( $21.4 \pm 2.8\%$ ) and ( $73.9 \pm 7.3\%$ ) for acetone and 2,2-dimethyl-propanal, respectively (Table 3). A previous FEP Teflon chamber study at ambient temperature and atmospheric pressure<sup>42</sup> reported formation yields of ( $19 \pm 1\%$ ) and ( $84 \pm 4\%$ ) for acetone and 2,2-dimethyl-propanal, respectively, in excellent agreement with our work.

The experimental results are supportive of the general Criegee mechanism for alkene ozonolysis, in agreement with the literature,<sup>42–45</sup> which consists in the concomitant formation of primary carbonyl compounds (2,2-dimethyl-propanal and acetone in the case of tM2P ozonolysis), and other stable oxidized reaction products from the Criegee intermediates such as hydroxy-acetone, methyl glyoxal, and formaldehyde. The dual-energy-rich Criegee radicals can follow collision-stabilization processes or unimolecular decomposition processes<sup>42,43,46</sup> to become low energy chemical entities. When the biradical involves a *t*-butyl substituent, intramolecular migration of a hydrogen atom leading to the formation of a hydroperoxide is not possible, thus implying the absence of hydroxy-carbonyl and  $\alpha$ -dicarbonyl products.<sup>6</sup>

In addition to the primary reaction products, the study identified and quantified a nonoxidized product, 2-methyl-1-propene, with an average contribution of ( $11.9 \pm 2.4\%$ ), and the profiles are reported in Table 3 and Figure 7 for different reaction rates. A new reaction mechanism is proposed involving



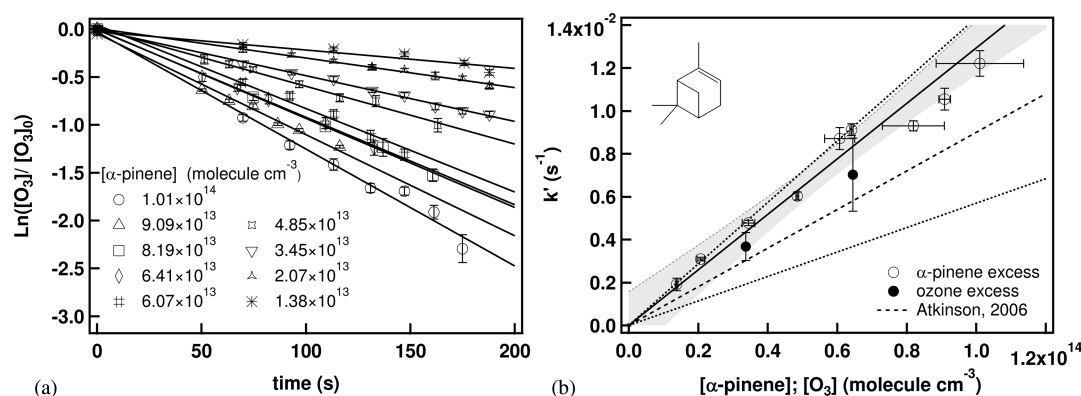


**Figure 6.** Kinetics of  $\alpha$ -pinene ozonolysis. (a) Plots of ozone consumption versus time (excess of  $\alpha$ -pinene). (b) Plot of the pseudo-first-order rate coefficient  $k'_{\text{ALK}}$  versus alkene concentration (excess of  $\alpha$ -pinene, open circles) or versus ozone concentration (excess of ozone, filled circles) and comparison with the IUPAC recommendation<sup>40</sup> (dotted line). The straight line is the linear regression fit, and the gray area represents the 95% confidence interval. The dashed lines represent the uncertainty limits given by the IUPAC (i.e.,  $5.7$  and  $14.3 \times 10^{-17} \text{ cm}^3 \text{ molecule}^{-1} \text{ s}^{-1}$ ).

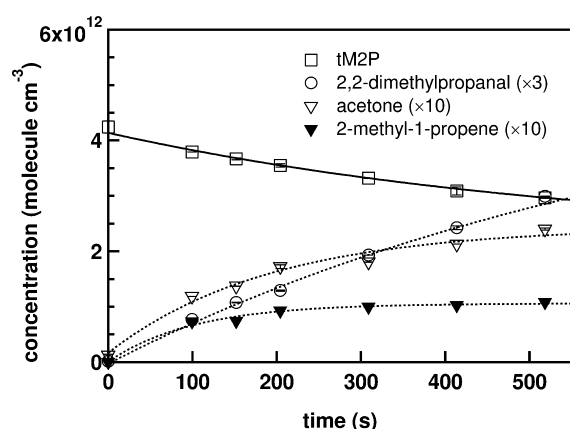


**Figure 7.** Time profiles of the tM2P ozonolysis products in the gas phase in presence of an OH scavenger. Lines in the figure are drawn to guide the eye and do not represent a model fit.

electron rearrangement in the Criegee intermediate containing the *t*-butyl substituent, with the formation of OH and HCO radicals and a nonoxidized alkene: 2-methyl-1-propene (Figure 8). Its formation yields present a lowering tendency with reaction time, suggesting competitive reactions of ozone (since OH radicals are scavenged by CO) with either the formed alkene or tM2P, and they remain invariably below the formation yields of acetone, which is the molecule formed simultaneously in the suggested Criegee reaction mechanism. The two expected stable products from the ozonolysis reaction of 2-methyl-1-propene are acetone and formaldehyde.

**2.4. Structure–Activity Relationship Analysis.** An SAR analysis based on the data from the present study (Table 2) and literature data (Table 4) was applied to check the consistency of the obtained rate coefficients. Different approaches are

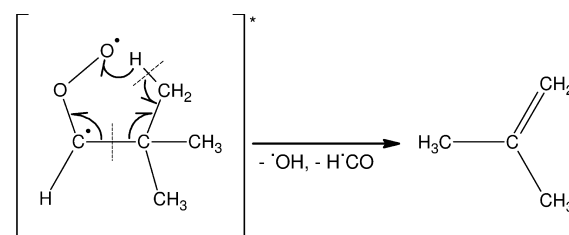


**Figure 8.** Suggested mechanism for the formation of 2-methyl-2-propene via the Criegee intermediate.

presented in the literature regarding the SAR analysis for alkene ozonolysis, involving quantum molecular orbital calculations<sup>47</sup> or the topological SAR method.<sup>48</sup> The second method was chosen, as it seems to present a robust molecular approach for the estimation of the alkene ozonolysis kinetics, and the most accurate in the prediction of the rate coefficients.

The topological SAR methodology used is based on the influence of the structure of the molecule over the alkene reactivity in the ozonolysis process and is described in detail elsewhere.<sup>48</sup> The calculation of the ozonolysis rate coefficient is based on the estimation of the inductive (I) and steric (S) effects around the unsaturated bond for each molecule and is characterized by the index  $x$  calculated as

$$x = (\gamma S) + I \quad (\text{VIII})$$

where  $\gamma$  is an empirical constant and is equal to  $-4.04$ . On the basis of the analysis of a series of  $\text{C}_2$ – $\text{C}_{10}$  alkenes, McGillen et al. (2008)<sup>48</sup> derived the following correlation between the logarithm of the room temperature rate coefficient  $k_{\text{ALK}}$  and the SAR index  $x$ :  $\log k_{\text{ALK}} = (1.28 \pm 0.05)x - (18.14 \pm 0.07)$ .

**Table 3.** tM2P Ozonolysis Reaction: Alkene Consumption and Product Formation Yields for Different Reaction Times

reaction time (s)	$\Delta[\text{tM2P}]$ ( $10^{11}$ molecules $\text{cm}^{-3}$ )	acetone yield (%)	2,2-dimethyl-propanal yield (%)	$\Sigma$ branching ratios (%)	2-methyl-1-propene yield (%)
152	5.28	23.6	67.1	90.7	14.1
204	6.37	25.1	66.8	91.9	14.5
309	8.49	19.8	75.3	95.1	11.8
414	10.6	18.9	75.9	94.8	9.7
518	11.7	19.4	84.5	103.9	9.2
average yield (%)		$21.4 \pm 2.8$	$73.9 \pm 7.3$	$95.3 \pm 5.2$	$11.9 \pm 2.4$
Grosjean and Grosjean (1997) <sup>42</sup>		$19 \pm 1$	$84 \pm 4$	$103 \pm 4$	

**Table 4. Ozonolysis Rate Coefficients Predicted by the Topological SAR Algorithm<sup>48</sup> Taking into Account Inductive (I) and Steric (S) Effects in the Estimation of the SAR Index ( $\alpha$ ) and Available in the Literature<sup>49</sup> by Averaging Values at  $297 \pm 3$  K, unless Stated Otherwise**

alkene	$k_{\text{literature}}$ ( $\times 10^{-18}$ cm <sup>3</sup> molecule <sup>-1</sup> s <sup>-1</sup> )	$k_{\text{predicted}}$ ( $\times 10^{-18}$ cm <sup>3</sup> molecule <sup>-1</sup> s <sup>-1</sup> )	I	S	$\alpha$
ethene	1.65	0.72	0	0.000	0.000
propene	10.7	13.8	1	0.000	1.000
propene, 2-methyl	12.5	25.5	2	0.196	1.208
1-butene	10.4	9.34	1	0.033	0.867
1-butene, 2-methyl	13.9	17.3	2	0.229	1.076
1-butene, 3-methyl	9.51	6.32	1	0.066	0.735
1-butene, 2,3-dimethyl	10.0 <sup>b</sup>	11.7	2	0.262	0.943
1-butene, 3,3-dimethyl	3.90 <sup>b</sup>	4.27	1	0.098	0.602
1-butene, 2,3,3-trimethyl	7.75	7.90	2	0.294	0.811
1-butene, 2-ethyl	10.9	11.7	2	0.262	0.943
1-butene, 3-methyl-2-(1-methylethyl)	3.02	5.34	2	0.327	0.678
2-butene, (Z)-	140	263	2	0.000	2.000
2-butene, (E)-	223	263	2	0.000	2.000
2-butene, 2-methyl	486	486	3	0.196	2.208
2-butene, 2,3-dimethyl	1200	899	4	0.392	2.417
1-pentene	9.57	7.37	1	0.053	0.787
1-pentene, 2-methyl	13.1	13.6	2	0.249	0.996
1-pentene, 3-methyl	3.80 <sup>b</sup>	4.99	1	0.086	0.655
1-pentene, 4-methyl	8.70 <sup>a</sup>	5.82	1	0.073	0.707
1-pentene, 2,3-dimethyl	5.12	9.22	2	0.281	0.863
1-pentene, 2,4,4-trimethyl	14.8 <sup>a</sup>	8.49	2	0.288	0.835
2-pentene, (Z)-	168	178	2	0.033	1.867
2-pentene, (E)-	237	178	2	0.033	1.867
2-pentene, 2-methyl	430 <sup>a</sup>	329	3	0.229	2.076
2-pentene, 3-methyl, (Z)-	465	329	3	0.229	2.076
2-pentene, 3-methyl, (E)-	563	329	3	0.229	2.076
2-pentene, 2,4,4-trimethyl	132 <sup>a</sup>	151	3	0.294	1.811
1-hexene	10.9	7.37	1	0.053	0.787
2-hexene, (Z)-	104	140	2	0.053	1.787
2-hexene, (E)-	182	140	2	0.053	1.787
2-hexene, 3,4-diethyl, (Z)-	3.99	93.8	3	0.334	1.650
3-hexene, (Z)-	144	120	2	0.066	1.735
3-hexene, (E)-	157	120	2	0.066	1.735
3-hexene, 2,5-dimethyl, (E)-	38.4	55.1	2	0.131	1.470
3-hexene, 2,2-dimethyl, (E)-	40.4	55.1	2	0.131	1.470
1-heptene	11.4	7.37	1	0.053	0.787
1-octene	12.5 <sup>b</sup>	7.37	1	0.053	0.787
4-octene, (Z)-	89.8	75.0	2	0.105	1.574
4-octene, (E)-	131 <sup>c</sup>	75.0	2	0.105	1.574
1-decene	8.00 <sup>b</sup>	7.37	1	0.053	0.787
5-decene, (Z)-	114	75.0	2	0.105	1.574
1-tetradecene	22.0	7.37	1	0.053	0.787
1,3-butadiene	6.57	13.8	2	0.000	1.000
isoprene	12.6	18.8	3	0.196	1.104
1,3-butadiene, 2,3-dimethyl	25.6	25.5	4	0.392	1.208
1,3-pentadiene, (Z)-	27.8	60.3	3	0.000	1.500
1,3-pentadiene, (E)-	43.2	60.3	3	0.000	1.500
1,3-pentadiene, 2-methyl	80.0	81.9	4	0.196	1.604
2,4-hexadiene, (Z, E)-	314	263	4	0.000	2.000
2,4-hexadiene, (E, E)-	374	263	4	0.000	2.000
1,4-pentadiene	14.5	13.8	2	0.000	1.000
1,4-pentadiene, 2-methyl	13.2	18.8	3	0.196	1.104
1,5-hexadiene, 2-methyl	20.7	10.0	3	0.301	0.891
1,5-Hexadiene, 2,5-dimethyl	14.2	25.5	4	0.392	1.208
2,4-hexadiene, 2,5-dimethyl	3060	486	6	0.392	2.208
1,3-hexadiene, 5-methyl	23.9	40.8	3	0.066	1.367
1,3-hexadiene, 5,5-dimethyl	25.3	33.5	3	0.098	1.301
1,6-octadiene, 3,7-dimethyl	691	36.0	4	0.334	1.325
$\alpha$ -pinene	90.0	46.1	3	0.394	1.409

<sup>a</sup>Averaged value between the literature data and the current study. <sup>b</sup>Values at 288 K. <sup>c</sup>Values at 290 K.

A series of alkenes and dialkenes ranging from C<sub>2</sub> to C<sub>14</sub> for which room temperature ozonolysis rate coefficients are available in the literature<sup>49</sup> were selected (Table 4). The alkenes included in the analysis were chosen on the grounds of similarity with the molecules used for the validation of the flow reactor, presenting an internal or a terminal double bond, various degrees of branching, and a wide range of ozonolysis rate coefficient values, spanning the range  $10^{-15}$  to  $10^{-18}$  cm<sup>3</sup> molecule<sup>-1</sup> s<sup>-1</sup>. Applying the correlation from McGillen et al. (2008) to the selected alkenes allowed calculating predicted O<sub>3</sub> rate coefficients, which, as reported in Table 4, present a general good agreement (within a factor spanning from 0.46 to 2.98) to the measured rate coefficients, including those determined in the present work.

Within the obtained data set of the 59 considered compounds, there are three statistical outliers presented in Figure 9 (crosses) but not taken into account for the estimation of the SAR correlation (open squares). It is worth noting that all estimated rates of ozonolysis of the outliers (1,6-octadiene, 3,7-dimethyl; 2-hexene, 3,4-diethyl, and 2,4-hexadiene, 2,5-dimethyl) are measured only once,<sup>49</sup> and various consistency problems for these data are observed.<sup>48</sup>

Additionally, using the literature data listed in Table 4 and our own values of rate coefficients, a new linear regression, using a larger set of data, of  $\log k_{\text{ALK}}$  as a function of  $\alpha$  could be obtained (Figure 9):

$$\log k_{\text{ALK}} = (1.26 \pm 0.10)\alpha - (18.10 \pm 0.14) \quad (\text{IX})$$

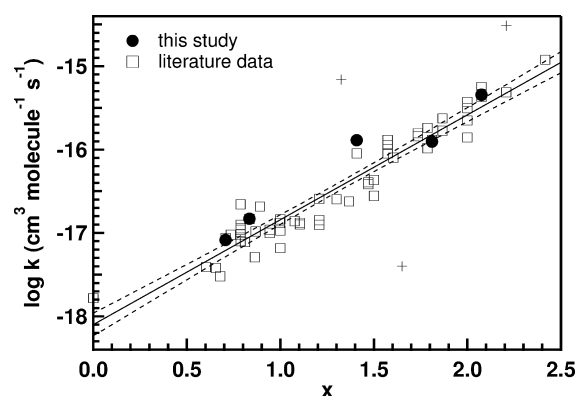


**Figure 9.** Ozonolysis rate coefficient (log scale) as a function of the SAR index  $x$  for the selected alkenes in Table 4 and the corresponding 95% confidence interval (dotted line). Filled circles: this work; open squares: literature data; crosses: outliers of literature data.

where the errors on the slope and the intercept are calculated for a 95% confidence interval, and a value of  $R^2 \sim 0.93$  has been obtained for the linear regression. This correlation (eq IX) is in excellent agreement with the one quoted by McGillen et al. (2008) who took into account a smaller database.

## CONCLUSION

The rate coefficients of the reactions of ozonolysis of four methylated pentenes and  $\alpha$ -pinene have been determined using a new flow tube reactor and a Teflon smog chamber. The results obtained have shown very good agreement with literature data, indicating that we may rely on the reactor to perform further kinetic studies on new systems.

The present measurements confirmed the strong increase of the ozonolysis rate coefficients with alkyl substitution at the double bond, probably due to the lowering of the ionization potential of the olefin, while substitution with a bulky substituent (such as *t*-butyl in tM2P) slightly reduces the reactivity through steric effects. The topological SAR analysis performed using the model of McGillen et al. (2008) provided an excellent correlation with existing data and confirms the consistency of the measured kinetic data.

The product yields determined in the tM2P ozonolysis study carried out in the flow reactor at short reaction times were in excellent agreement with the literature data and also allowed the identification of a new nonoxidized product (2-methyl-1-propene), probably derived from the electronic rearrangement of one Criegee intermediate. This strongly confirms the flow reactor suitability to carry out further similar studies and its potential to quantify reaction intermediates that are difficult to identify by smog chamber reactors because of their high reactivity, involving competitive formation and consumption.

In further studies, we will use readily available state-of-the-art instrumentation to characterize SOA by coupling a scanning mobility particle sizer (SMPS) to measure the number and size distribution of particles formed and a high-resolution time-of-flight aerosol mass spectrometer (HR-ToF-AMS) to determine their chemical average composition. The gas phase will be monitored both by online TD/GC/FID-MS and a proton-transfer-reaction time-of-flight mass spectrometer (PTR-ToF-MS) to try to identify more reactive intermediates.

## AUTHOR INFORMATION

### Corresponding Author

\*Phone: (33) 327 712 604; fax: (33) 327 712 914; e-mail: veronique.riffault@mines-douai.fr.

### Notes

The authors declare no competing financial interest.

## ACKNOWLEDGMENTS

Our laboratory participates in the Institut de Recherche en Environnement Industriel (IRENI), which is financed by the Communauté Urbaine de Dunkerque, the Nord-Pas de Calais Regional Council, the French Ministry of Higher Education and Research, the CNRS, and the European Regional Development Fund (ERDF). R.I.O. acknowledges the EMD and the IRENI for a 1-month Invited Professor Fellowship. M.D. is grateful for a Ph.D. scholarship from the Nord-Pas de Calais Regional Council and Armines.

## REFERENCES

- (1) Siese, M.; Becker, K. H.; Brockmann, K. J.; Geiger, H.; Hofzumahaus, A.; Holland, F.; Mihelcic, D.; Wirtz, K. *Environ. Sci. Technol.* **2001**, *35*, 4660–4667.
- (2) Atkinson, R.; Aschmann, S. M. *Environ. Sci. Technol.* **1993**, *27*, 1357–1363.
- (3) Aschmann, S. M.; Arey, J.; Atkinson, R. *Atmos. Environ.* **2002**, *36*, 4347–4355.
- (4) Grosjean, E.; Grosjean, D. *Environ. Sci. Technol.* **1996**, *30*, 2038–2044.
- (5) Grosjean, E.; Grosjean, D. *Atmos. Environ.* **1996**, *30*, 4107–4113.
- (6) Grosjean, E.; Grosjean, D. *Atmos. Environ.* **1998**, *32*, 3393–3402.
- (7) Hearn, J. D.; Smith, G. D. *J. Phys. Chem. A* **2004**, *108*, 10019–10029.
- (8) Stenby, C.; Pöschl, U.; von Hessberg, P.; Bilde, M.; Nielsen, O. J.; Moortgat, G. K. *Atmos. Chem. Phys. Discuss.* **2006**, *6*, 10275–10297.
- (9) Bonn, B.; Schuster, G.; Moortgat, G. K. *J. Phys. Chem. A* **2002**, *106*, 2869–2881.
- (10) Jang, M.; Lee, S.; Kamens, R. M. *Atmos. Environ.* **2003**, *37*, 2125–2138.
- (11) Czoschke, N. M.; Jang, M.; Kamens, R. M. *Atmos. Environ.* **2003**, *37*, 4287–4299.
- (12) Morris, J. W.; Davidovits, P.; Jayne, J. T.; Jimenez, J. L.; Shi, Q.; Kolb, C. E.; Worsnop, D. R.; Barney, W. S.; Cass, G. *Geophys. Res. Lett.* **2002**, *29*.
- (13) Ezell, M. J.; Johnson, S. N.; Yu, Y.; Perraud, V.; Bruns, E. A.; Alexander, M. L.; Zelenyuk, A.; Dabdub, D.; Finlayson-Pitts, B. J. *Aerosol Sci. Technol.* **2010**, *44*, 329–338.
- (14) Lee, S.; Kamens, R. M. *Atmos. Environ.* **2005**, *39*, 6822–6832.
- (15) Bilde, M.; Pandis, S. N. *Environ. Sci. Technol.* **2001**, *35*, 3344–3349.
- (16) Tolocka, M. P.; Heaton, K. J.; Dreyfus, M. A.; Wang, S.; Zordan, C. A.; Saul, T. D.; Johnston, M. V. *Environ. Sci. Technol.* **2006**, *40*, 1843–1848.
- (17) Schauer, J. J.; Kleeman, M. J.; Cass, G. R.; Simoneit, B. R. T. *Environ. Sci. Technol.* **1999**, *33*, 1578–1587.
- (18) Schauer, J. J.; Kleeman, M. J.; Cass, G. R.; Simoneit, B. R. T. *Environ. Sci. Technol.* **2001**, *35*, 1716–1728.
- (19) Hays, M. D.; Geron, C. D.; Linna, K. J.; Smith, N. D.; Schauer, J. J. *Environ. Sci. Technol.* **2002**, *36*, 2281–2295.
- (20) Pinho, P. G.; Pio, C. A.; Carter, W. P. L.; Jenkin, M. E. *J. Atmos. Chem.* **2006**, *55*, 55–79.
- (21) Kroll, J. H.; Seinfeld, J. H. *Environ. Sci. Technol.* **2005**, *39*, 4159–4165.
- (22) Kroll, J. H.; Seinfeld, J. H. *Atmos. Environ.* **2008**, *42*, 3593–3624.
- (23) Bennadji, H.; Glaude, P. A.; Coniglio, L.; Billaud, F. *Fuel* **2011**, *90*, 3237–3253.

- (24) Seeley, J. V.; Jayne, J. T.; Molina, M. J. *Int. J. Chem. Kinet.* **1993**, *25*, 571–594.
- (25) Helmig, D. *Atmos. Environ.* **1997**, *31*, 3635–3651.
- (26) Turpin, E.; Tomas, A.; Fittschen, C.; Devolder, P.; Galloo, J.-C. *Environ. Sci. Technol.* **2006**, *40*, 5956–5961.
- (27) Malkin, T. L.; Goddard, A.; Heard, D. E.; Seakins, P. W. *Atmos. Chem. Phys.* **2010**, *10*, 1441–1459.
- (28) Kroll, J. H.; Clarke, J. S.; Donahue, N. M.; Anderson, J. G.; Demerjian, K. L. *J. Phys. Chem. A* **2001**, *105*, 1554–1560.
- (29) Kroll, J. H.; Donahue, N. M.; Cee, V. J.; Demerjian, K. L.; Anderson, J. G. *J. Am. Chem. Soc.* **2002**, *124*, 8518–8519.
- (30) Tuazon, E. C.; Aschmann, S. M.; Arey, J.; Atkinson, R. *Environ. Sci. Technol.* **1997**, *31*, 3004–3009.
- (31) Hasson, A. S.; Chung, M. Y.; Kuwata, K. T.; Converse, A. D.; Krohn, D.; Paulson, S. E. *J. Phys. Chem. A* **2003**, *107*, 6176–6182.
- (32) Rickard, A. R.; Johnson, D.; McGill, C. D.; Marston, G. J. *J. Phys. Chem. A* **1999**, *103*, 7656–7664.
- (33) Presto, A. A.; Donahue, N. M. *J. Phys. Chem. A* **2004**, *108*, 9096–9104.
- (34) Gutbrod, R.; Meyer, S.; Rahman, M. M.; Schindler, R. N. *Int. J. Chem. Kinet.* **1997**, *29*, 717–723.
- (35) Horie, O.; Moortgat, G. K. *Chem. Phys. Lett.* **1998**, *288*, 464–472.
- (36) Grosjean, E.; Grosjean, D. *Int. J. Chem. Kinet.* **1995**, *27*, 1045–1054.
- (37) Leather, K. E.; McGillen, M. R.; Percival, C. J. *J. Phys. Chem. Chem. Phys.* **2010**, *12*, 2935–2943.
- (38) Atkinson, R.; Carter, W. P. L. *Chem. Rev.* **1984**, *84*, 437–470.
- (39) Grosjean, E.; Grosjean, D. *Int. J. Chem. Kinet.* **1996**, *28*, 911–918.
- (40) Atkinson, R.; Baulch, D. L.; Cox, R. A.; Crowley, J. N.; Hampson, R. F.; Haynes, R. G.; Jenkin, M. E.; Rossi, M. J.; Troe, J. *Atmos. Chem. Phys.* **2006**, *6*, 3625–4055.
- (41) Bernard, F.; Fedioun, I.; Peyroux, F.; Quilgars, A.; Daële, V.; Mellouki, A. *J. Aerosol Sci.* **2012**, *43*, 14–30.
- (42) Grosjean, E.; Grosjean, D. *Environ. Sci. Technol.* **1997**, *31*, 2421–2427.
- (43) Finlayson-Pitts, B. J.; Pitts, J. N. *J. Chemistry and Physics of the Upper and Lower Atmosphere*; Wiley: New York, 1999.
- (44) Neeb, P.; Moortgat, G. K. *J. Phys. Chem. A* **1999**, *103*, 9003–9012.
- (45) Seinfeld, J. H.; Pandis, S. N. *Atmospheric Chemistry and Physics: From Air Pollution to Climate Change*; Wiley: New York, 1998; Vol. 2.
- (46) Horie, O.; Moortgat, G. K. *Acc. Chem. Res.* **1998**, *31*, 387–396.
- (47) King, M. D.; Canosa-Mas, C. E.; Wayne, R. P. *J. Phys. Chem. Chem. Phys.* **1999**, *1*, 2231–2238.
- (48) McGillen, M. R.; Carey, T. J.; Archibald, A. T.; Wenger, J. C.; Shallcross, D. E.; Percival, C. J. *J. Phys. Chem. Chem. Phys.* **2008**, *10*, 1757–1768.
- (49) NIST. Chemical Kinetics Database on the Web. In *Standard Reference Database 17, Version 7.0(Web Version)*, Release 1.6.0; 7.0 ed., 2011.
- (50) Cox, R. A.; Penkett, S. A. *J. Chem. Soc., Faraday Trans. 1* **1972**, *68*, 1735–1753.